blood

Prepublished online September 24, 2012;
doi:10.1182/blood-2012-07-442277

Human red blood cells at work: identification and visualization of erythrocytic eNOS activity in health and disease

Miriam M. Cortese-Krott, Ana Rodriguez-Mateos, Roberto Sansone, Gunter G.C. Kuhnle, Sivatharsini Thasian-Sivarajah, Thomas Krenz, Patrick Horn, Christoph Krisp, Dirk Wolters, Christian Heiß, Klaus-Dietrich Kröncke, Neil Hogg, Martin Feelisch and Malte Kelm

Blood (print ISSN 0006-4971, online ISSN 1528-0020), is published weekly by the American Society of Hematology, 2021 L St, NW, Suite 900, Washington DC 20036.

RED CELLS, IRON, AND ERYTHROPOIESIS

Human red blood cells at work: identification and visualization of erythrocytic eNOS activity in health and disease

Miriam M. Cortese-Krott[1], Ana Rodriguez-Mateos[3], Roberto Sansone[1], Gunter GC Kuhnle[3], Sivatharsini Thasian-Sivarajah[1], Thomas Krenz[1], Patrick Horn[1], Christoph Krisp,[4] Dirk Wolters,[4] Christian Heiß[1], Klaus-Dietrich Kröncke[2], Neil Hogg[5], Martin Feelisch[6], Malte Kelm[1]

[1]Cardiovascular Research Laboratory, Department of Cardiology, Pulmonology and Angiology;
and [2]Institute of Biochemistry and Molecular Biology I, Medical Faculty, Heinrich Heine University of Düsseldorf, Moorenstr.5, 40225 Düsseldorf, Germany.
[3]Department of Food and Nutritional Sciences, University of Reading, Whiteknights, Reading RG6 6AD, UK.
[4]Biomolecular Mass Spectroscopy/Protein Center, Department of Analytical Chemistry, Ruhr-University Bochum, Germany.
[5]Department of Biophysics, Medical College of Wisconsin, Milwaukee, Wisconsin, USA
[6]University of Southampton, Clinical & Experimental Sciences, Faculty of Medicine, Southampton General Hospital, Southampton, UK

Corresponding author:

Malte Kelm, MD
Department of Cardiology, Pulmonology, and Vascular Medicine
Medical Faculty, Heinrich-Heine-University of Düsseldorf,
40225 Düsseldorf, Moorenstr. 5, Germany.
Tel. +49 (0) 211 811 8801
Fax. +49 (0) 211 811 8812
malte.kelm@med-uni.duesseldorf.de

Abstract

A nitric oxide synthase (NOS)-like activity has been demonstrated in human red blood cells (RBCs), but doubts about its functional significance, isoform identity and disease relevance remain. Using flow cytometry in combination with the NO-imaging probe DAF-FM we find that all blood cells form NO intracellularly, with a rank order of monocytes > neutrophils > lymphocytes > RBCs > platelets. The observation of a NO-related fluorescence within RBCs was unexpected given the abundance of the NO-scavenger oxyhemoglobin. Constitutive normoxic NO formation was abolished by NOS inhibition and intracellular NO scavenging, confirmed by laser-scanning microscopy and unequivocally validated by detection of the DAF-FM reaction product with NO using HPLC and LC-MS/MS. Employing immunoprecipitation, ESI-MS/MS-based peptide sequencing and enzymatic assay we further demonstrate that human RBCs contain an endothelial NOS (eNOS) that converts L-^{3}H-Arginine to L-^{3}H-Citrulline in a Ca^{2+}/Calmodulin-dependent fashion. Moreover, in patients with coronary artery disease, red cell eNOS expression and activity are both lower than in age-matched healthy individuals and correlate with the degree of endothelial dysfunction. Thus, human RBCs constitutively produce NO under normoxic conditions via an active eNOS isoform the activity of which is compromised in patients with coronary artery disease.

Title page notes

Part of this work has been presented in abstract form at the Joint meeting of the societies of free radical biology and medicine and the free radical research international, Orlando, (FL, USA) November 2010 and Atlanta, (GE, USA) November 2011.

The online version of the article contains a data supplement.

Introduction

The key event in the pathogenesis of arteriosclerosis is believed to be a dysfunction of the endothelium with disruption of vascular homeostasis, predisposing blood vessels to vasoconstriction, inflammation, leukocyte adhesion, thrombosis, and proliferation of vascular smooth muscle cells. Red blood cells (RBCs) are typically considered as shuttles of respiratory gases and nutrients for tissues, less so as compartments important to vascular integrity. Patients with coronary artery disease (CAD) and concomitant anemia have a poorer prognosis following myocardial infarction, percutaneous coronary intervention, and coronary artery bypass grafting, and are more prone to developing heart failure with fatal outcomes [1-3]. Surprisingly, erythropoietin treatment fails to improve diagnosis, indicating that a compromised gas exchange/nutrient transport capacity of blood is insufficient to explain this outcome.

Nitric oxide (NO) is an essential short-lived signaling/regulatory product of a healthy endothelium that is critically important for vascular health. Decreased production and/or bioactivity of NO are a hallmark of endothelial dysfunction and have been shown to contribute to accelerated atherogenesis. In the cardiovascular system, NO is continuously produced in endothelial cells by the type III isoform of NO synthase (eNOS, NOS3; EC 1.14.13.39)[4]. In addition to endothelial cells, some circulating blood cells also contain eNOS.

It is an accepted dogma that RBCs take up and inactivate endothelium-derived NO via rapid reaction with oxyhemoglobin to form methemoglobin and nitrate, thereby limiting NO available for vasodilatation. Yet it has also been shown that RBCs not only act as “NO sinks” but synthesize, store, and transport NO metabolic products. Under hypoxic conditions in particular, it has been demonstrated that RBCs induce NO-dependent vasorelaxation.[5;6] Mechanisms of release and potential sources of NO in RBCs are still a matter of debate, but candidates include iron-nitrosyl-hemoglobin[7], S-nitrosohemoglobin[8-10], and nitrite. The latter may form NO either via deoxyhemoglobin[5;11] or xanthine oxidoreductase (XOR)-mediated reduction[6;12], or via spontaneous[12] and carbonic anhydrase-facilitated disproportionation[13]. Most of these processes show a clear oxygen-dependence, and several are favoured by low

oxygen tensions. The relative contribution of either mechanism to NO formation varies with oxygen partial pressure along the vascular tree. In addition, RBCs release ATP when subjected to hypoxia, providing an alternative vasodilatory pathway[14].

In contrast to hypoxia-induced NO release from RBCs, their generation of NO under normoxic conditions is less well characterized. Data from our and other laboratories have demonstrated a NOS-dependent NO production from RBCs in normoxia, suggesting RBCs may contribute to the inhibition of platelet aggregation[15;16], the circulating pool of NO metabolites[15-18], and to overall tissue protection[17;18]. Treating RBCs with NOS inhibitors decreased accumulation of NO metabolites[16;19] and citrulline [15;18] in the supernatant. However, Kang *et al.* failed to measure citrulline production in RBC lysates[20], maybe because of loss of cellular structures or cofactors important for activity[21].

Another recent study failed to detect increases in ^{15}N-labelled nitrite/nitrate following addition of ^{15}N-L-Arg to intact RBCs[22]. RBCs have been shown to express a protein containing epitopes of an eNOS[6;15;16;20;23-25]. However, positive staining with anti-iNOS antibodies has also been reported[20;25], and others suggested that RBCs might express a novel NOS isoform.[23;25] Thus, doubts about the functional significance of the NOS-like activity in RBCs remain, and little is known about NOS isoform identity and disease relevance.

We therefore sought to definitively identify and characterize the activity of human red cell NOS using an advanced multilevel analytical approach. Using HPLC, LC-MS/MS, flow cytometry, laser scanning microscopy and enzymatic assay together with functional studies we here demonstrate that human RBCs contain an active eNOS that gives rise to constitutive intracellular NO formation under normoxic conditions. We further show that this activity is compromised in CAD and correlates with the degree of endothelial dysfunction.

Materials and methods

Study subjects

Blood drawn from human healthy subjects (25-33 ys) was used for biochemical characterization of human red cell eNOS. To compare NOS expression with vascular function, 10 patients with endothelial dysfunction due to coronary artery disease (CAD), as diagnosed by coronary angiography, and 9 age-matched healthy subjects were recruited from the outpatient clinic of the Department of Cardiology, Pulmonology and Angiology, Düsseldorf University Hospital. NOS activity was quantified in red cells from a randomized subset of the study population composed of 4 healthy individuals and 5 patients with CAD. All subjects provided written informed consent before enrollment. Procedures were conducted in accordance with the Declaration of Helsinki and approved by the local ethics committee of the Heinrich-Heine University of Düsseldorf. Endothelium-dependent dilation of the brachial artery was assessed non-invasively by measurement of flow-mediated dilatation (FMD) using high-resolution ultrasound (VIVID i, GE Healthcare)[26]. FMD and endothelium-independent dilation were expressed as a percentage change from baseline. See supplemental methods for further details.

Comparative flow cytometric analysis of blood cells

Three aliquots of blood were processed for analysis of leukocytes, RBC and platelets, as described in supplemental methods. Briefly, each aliquot was loaded with 10 µM DAF-FM diacetate for 30 min at RT in the dark, or left untreated, washed in PBS and analyzed for DAF FM-associated fluorescence in a FACS Canto II flow cytometer. NO donors were applied to RBC preparations at the indicated concentrations after washing the DAF-FM-loaded cells. For NOS inhibition, RBC suspensions were pre-incubated for 30 min with 3 mM L-NAME or 1 mM L-NIO. Intracellular NO was scavenged by incubation of RBC suspensions for 30 min at 37°C with 250 µM iron diethyldithiocarbamate ($Fe[DETC]_2$) prepared as described,[27] and then washed by centrifugation at 300xg for 10 min at 4°C. Aliquots from these preparations were analyzed within 15 min in a FACS Canto II flow cytometer after

further 1:3 dilution in PBS. Flow cytometric data were collected using the DIVA 5.0 software package and analyzed using FlowJo V7.5.5 (TreeStar). Median fluorescence intensity (MFI) was calculated from the histogram (distribution) plots of the green fluorescence signals (Ex 488 nm, Em 530±30 nm) detected within the cell-specific gates (see Fig. 1A-C, panels I, gated cells are color-coded). MFIs of untreated samples served as autofluorescence controls. The acquisition voltage was adjusted before each measurement according to the position of the third fluorescence peak of standard latex beads (Rainbow beads, BD Bioscience).

Visualization of DAF-FM fluorescence in RBC by laser-scanning microscopy

Whole blood was diluted 1:10 in PBS and treated with 10-30 µM DAF-FM diacetate for 30 min at RT or 37°C in the dark, washed and treated with 100 µM Spermine/NO (Sper/NO), or 100 µM S-nitrosocysteine (SNOC) for 15 min. Unstained cells served as autofluorescence controls. Blood smears were analyzed 1-5 min after preparation under a Zeiss LSM 510 confocal laser-scanning microscope using a Zeiss Plan Neofluar 63x/1.3 oil DIC objective and excitation (Ex) 488 nm with UV/488/543/633 nm beam splitter. Fluorescence was recorded using a 540-30 nm bandpass filter and micrographs were taken at 37°C. Images were processed with Adobe Photoshop CS5 (Adobe Systems GmbH).

HPLC analysis of the nitrosation products of DAF-FM

Red cell pellets were diluted 1:500 in PBS, pre-treated as described in the flow cytometry section, washed, and loaded by 30 min incubation with 10 µM DAF-FM diacetate at RT in the dark. After centrifugation at 300xg for 10 min at 4°C, pellets were incubated with HPLC-grade DMSO for 30 min at RT in the dark and spun down at 13,000xg for 10 min. The supernatants were analyzed by reversed-phase high performance liquid chromatography (HPLC) applying a method described for DAF-2[28] with some modifications, using an Agilent 1100 Series HPLC system (Agilent Technologies) with a diode array detector (set to 490 nm) and a fluorescence detector (Ex 490, Em 517) connected in series. The column used was a Phenomenex Luna C18 (2) (4.6 x 250 mm; 5 µm) fitted with a guard column, both

kept at 25°C. The mobile phase consisted of 0.05% TFA in water (A) and 0.05% TFA in acetonitrile (B), using the following gradient settings (time/%A): 0 min-95%, 40 min-60%, 45 min-60% with a flow rate of 1 ml/min.

Identification of DAF-FM reaction products by LC-MS/MS

Mass spectra were run on an Agilent 6400 triple-quadrupole liquid chromatography mass spectrometry (LC-MS/MS) instrument operated in positive ion mode; samples were separated using a Kinetix C18(2) column (2 x 50 mm; Phenomenex) with 0.1% aqueous formic acid (A) and methanol (B) as mobile phase (flow rate 200 µL/min, gradient [time, %A]: 0 min-80%, 1 min-80%, 2.1 min-30%. 3.1 min-30%, 3.5 min 80%, 5 min-80%). DAF-FM (transition 413.2 → 369.12) and DAF-FM-T (transition 424.2 → 380.1) were detected using selective-reaction monitoring.

Immunoprecipitation, gel electrophoresis and western blot analysis

Crude protein extract was obtained by lysis of RBC pellets (1 ml) with toluene[29]. EC were lysed as described[30]. Total protein concentration was determined by Lowry (DC Protein Assay, Bio-Rad). Probes (100 µg/µl protein) were incubated for 1 h at RT with a mouse anti-human NOS3 antibody (40 µg, BD Bioscience). Immunocomplexes were isolated by magnetic separation using protein G Dynabeads (Invitrogen) following the manufacturer's instruction. For gel electrophoresis, samples were loaded onto 7% NuPAGE Novex Tris/Acetate pre-cast gels (Invitrogen), and protein bands were stained with colloidal Coomassie Brilliant Blue[31]. Western blot analysis was performed as previously described[30]using rabbit anti-NOS3 antiserum (BD Bioscience) (1:1000) and HRP-conjugated goat anti-rabbit antibody (1:5000 Rockland).

Peptide sequencing by ESI-MS/MS

In-gel digestion and peptide separation was performed as described in supplemental methods. Eluting ions were transferred directly into a LTQ XL linear ion trap mass spectrometer (Thermo Fisher Scientific) equipped with an electrospray ionization device (spray voltage 1.8 kV, capillary temperature 180°C). Precursor ions were detected in a full

MS scan from 400 to 2000 m/z. Full MS/MS spectra were acquired for the 10 most intense signals using a fill time of 100 ms for each MS/MS µscan. MS/MS spectra were interpreted with the SEQUEST algorithm implemented in the Proteome Discoverer software (Thermo Fisher Scientific) and searched against the human Swiss-Prot database (release 15.6/57.6). Peptide mass accuracy for precursor ions and tolerance for fragment ions were respectively set to 2.5 and to 1 atomic mass units, allowing methionine oxidation as a possible chemical modification.

Peptide alignments

Peptide sequences were aligned with the sequences of all main NOS isoforms and eNOS splice variants using the constraint-based multiple alignment tool (COBALT) of the NCBI website (protein accession numbers NP_000611 = NOS1, nNOS; NP_000616= NOS2, iNOS; NP_000594 = NOS3, isoform 1; with splicing variants of NOS3 as NP_001153581 = NOS3, isoform 2, NP_001153582 = NOS3, isoform 3, and NP_001153583 = NOS3, isoform 4). The position of the peptides in the conserved regions were visualized using Geneious v5.4 software (Biomatters Ltd).

Determination of NOS activity

The activity of the immunoprecipitated protein was determined by measuring the rate of conversion (fmol/min) of [^{3}H] L-arginine to [^{3}H] citrulline or [^{14}C] L-arginine to [^{14}C] citrulline as previously described[32], in the presence or absence of the specific NOS inhibitors L-NAME (1 mM each), or of Ca^{2+} (75 µM) + calmodulin (0.04 µg/µl) (see supplemental methods for details).

Results

RBCs loaded with DAF-FM are fluorescent

To compare intracellular NO production between circulating blood cells, blood fractions enriched in leukocytes, platelets and erythrocytes were loaded with DAF-FM diacetate and analyzed by flow cytometry (Fig. 1). Individual cell subpopulations were identified by staining with specific surface markers and by analysis of scatter dot plots (Fig. 1A-C, panels I). Monocytes revealed the highest intracellular fluorescence intensity, followed by neutrophils, lymphocytes, RBCs, and platelets (Fig 1D). Whether these variations are due to differences in NO and/or reactive oxygen species (ROS) production, or dye uptake/processing remains to be investigated.

A DAF-FM-related fluorescence signal in RBCs was unexpected given the abundance of the NO scavenger oxyhemoglobin and the nitrosation scavengers glutathione and ascorbate in these cells. However, these original findings were confirmed by laser scanning microscopy (Fig. 2A). DAF-FM-associated fluorescence was remarkably uniform with a typical doughnut-shaped fluorescence pattern, and strongly increased following addition of the NO donors Sper/NO (Fig 2A bottom panel) or S-nitrosocysteine. Fluorescence intensity varied up to 5-fold between cells of the same preparation (see histogram plot in Fig. 1B, panel I and Fig. 2B), was sensitive to changes in incubation temperature (37°C >> RT), and oxygen tension (21% O_2 > 5% O_2). Median fluorescence intensity (MFI) increases were markedly (20-70%) inhibited by either pre-incubation of cells with the NOS-inhibitors, L-NAME (Fig. 2C) and L-NIO (n=6, p=0.048 vs. untreated control), or the lipophilic NO scavenger $Fe[DETC]_2$ (Fig. 2D). This degree of inhibition is probably maximal considering the strong background fluorescence due to the formation of unspecific fluorescent adducts[33] and the presence of fluorescence impurities in the DAF-FM DA stock solution (see below). Moreover, treating RBC with nitrite did not affect DAF-FM-dependent signal under neutral conditions, while at pH 5.5 only higher concentrations of nitrite (> 200 µM) strongly increased intracellular fluorescence (data not shown).

Unexpectedly, MFI did not increase upon addition of L-arginine (3 mM) to intact cells. These findings are consistent with the lack of ^{15}N-nitrite/nitrate production following incubation of RBCs with exogenous ^{15}N-L-Arg[34] and indicate that constitutive red cell NOS activity does not rely on extracellular substrate supply. By contrast, treatment with the nitrosating NO donor SNOC markedly increased fluorescence intensity in a concentration-dependent manner (Fig 2B) and this was inhibited by addition of $Fe[DETC]_2$ as assessed by fluorimetry (not shown). Intermediate SNOC concentrations produced fluorescence intensity distributions distinct from those at other concentrations, suggesting cell-to-cell differences in SNOC uptake and/or metabolism (Fig. 2B). Peak MFIs at maximal NO donor concentrations were similar and cell-to-cell variations small, indicative of comparable DAF-FM loading efficiencies. Thus fluorescence intensity variations at baseline likely reflect differences in constitutive NOS activity between cells. None of these treatments affected RBC morphology, as assessed in the transmitted light channel of the laser scanning microscope and by the lack of positional changes for the RBC population in the scatter dot plot using flow cytometry. Qualitatively identical results were obtained using fluorimetry (not shown). While no changes in cell morphology or hemolysis were observed with these treatments at the concentrations used (which could have impeded flow cytometric analysis), a high NO/NOS-independent background signal was apparent using these techniques, even after correction for autofluorescence.

DAF-FM-related fluorescence in RBCs originates from reaction with NOS-derived NO

To confirm that the fluorescent signals detected by fluorimetry, laser scanning microscopy and flow cytometry were indeed due to intracellular nitrosation of DAF-FM to form DAF-FM-T, we analyzed the products of this reaction by HPLC and LC-MS/MS. A peak corresponding to DAF-FM-T was detected in loaded RBCs by reversed phase HPLC (Fig 3A). Combined use of selected reaction monitoring (i.e., multiple reaction monitoring of the 413.1$\rightarrow$369.1 and 424.1$\rightarrow$380.1 transitions) by LC-MS/MS in parallel with HPLC allowed us to detect both DAF-FM-T and unreacted DAF-FM in RBCs pre-loaded with DAF-FM diacetate, thus providing unequivocal evidence for formation of DAF-FM-T and, therefore, constitutive NO

production within RBCs (Fig 3B). Reassuringly, no peak corresponding to DAF-FM-T was detected in RBCs pre-treated with either the NOS inhibitor, L-NAME (Fig. 3A, panel II; Fig. 3C 10 out of 12 samples; n=5 independent experiments) or the lipophilic NO scavenger, $Fe[DETC]_2$ (Fig 3A, panel III; Fig. 3D). Fluorescence quenching effects of the dark-colored $Fe[DETC]_2$ can be excluded because excess compound was removed by the washing steps before DAF-FM-T extraction.

When plotting the area of the fluorescent peaks obtained by serial dilution of DAF-FM-T standards in RBC lysates against triazole concentration (assuming 100% conversion efficiency of DAF-FM authentic standard into DAF-FM-T by reaction with SNOC) a linear relationship was apparent (Fig 3E; $R = 0.9989$; $p<0.0001$). By interpolating the areas of the DAF-FM-T related peaks observed in $1.2x10^7$ DAF-FM-loaded RBCs under basal conditions, we estimated that the average concentration of DAF-FM-T in these samples was 64±12 nM (n=19). Assuming the reaction stoichiometry to be 1:1, the amounts of NO and/or nitrosating equivalents produced by a single RBC within 30 min at RT corresponds to at least $3.2x10^{-6}$ fmoles (Fig. 3F).

RBCs contain the "classical" eNOS isoform

Having identified an intracellular constitutive NOS activity in RBCs, we next sought to isolate and identify the NOS isoform expressed in these cells. Crude hemolysates were prepared by osmotic lysis of RBC pellets with toluene/H_2O 1:1, which preserves protein structure and activity and avoids excessive dilution. We succeeded in immunoprecipitating an eNOS-like protein employing a mouse monoclonal anti-eNOS antibody, either after enrichment of calmodulin-binding proteins by affinity chromatography (Fig. 4A, lanes 1+2) or directly from crude red cell lysates (Fig. 4A, lanes 3+4; Fig 4B). After separation of the proteins by SDS-PAGE under reducing conditions followed by coomassie staining, a band of ~130kD was apparent in all samples (Fig 4A). The identity of this 130kD band was confirmed by Western blotting using a polyclonal rabbit anti-human eNOS antibody (Fig. 4B). Similar results were obtained by using the rabbit antibody for immunoprecipitation and the mouse antibody for detection, as well as by staining the membrane with a mouse monoclonal anti-eNOS

antibody directed against a different epitope of eNOS. No high-molecular-weight bands were detected if a mouse anti-human iNOS antibody was used for immunoprecipitation, or by adding antibodies and beads to a serum albumin solution.

To identify the immunoprecipitated protein(s), the 130kD bands of two independent coomassie-stained gels were excised (one of them shown in Fig 4C) and subjected to analysis by liquid chromatography-mass spectrometry (LC-MS/MS). Four different peptides all belonging to eNOS were identified. By alignment of the sequences of these peptides with those of the three NOS isoforms including all known splice variants of eNOS, we found that the identified peptides belong to two distinct, highly conserved regions of the reductase domain of the NOS protein (Fig. 4 D): the FMN reductase-like region (peptides 1 and 2) and the ferredoxin reductase (FNR)-like region (peptides 3 and 4) within the FAD-binding pocket (Fig. 4D). All four peptide sequences showed 100% pairwise identity only with the full eNOS sequence, with peptides 3 and 4 aligning within a region in the C-terminal domain that is absent in the truncated splice variants. Thus, these results show that human RBCs carry a NOS3, the “classical” eNOS isoform constitutively expressed in endothelial cells.

Isolated red cell eNOS protein is catalytically active

To verify that the erythrocytic eNOS identified is indeed active we measured the ability of the immunoprecipitated protein to catalyze the *in vitro* conversion of ^{3}H-L-arginine to ^{3}H-citrulline in the presence of NADPH, FAD, FMN, Ca^{2+} and calmodulin. Fig. 4E depicts the results from 5 independent experiments (ANOVA $p< 0.05$). We found that the protein is capable of producing 9.82 fmol/min citrulline under optimal substrate/cofactor supply conditions. Moreover, arginine to citrulline conversion was significantly inhibited by addition of the NOS inhibitor L-NAME (Fig 4E, IP vs. IP+L-NAME $p<0.05$) and markedly decreased in the absence of Ca^{2+}/calmodulin (Fig. 4E IP vs. IP w/o Ca^{++}/CaM; t-test $p<0.05$). Thus, the isolated eNOS is active and dependent on Ca^{2+}/calmodulin interaction.

Red cell eNOS expression and activity are compromised in patients with coronary artery disease

We explored endothelial function and erythrocytic eNOS expression levels and activity in patients with CAD, a condition associated with endothelial dysfunction, and age-matched healthy individuals. Clinical characteristics of the study population are summarized in Table S1. As expected, flow-mediated dilation of the brachial artery was significantly decreased in CAD patients, while maximal vasodilatation in response to GTN was not significantly different (Table S1). Patients with endothelial dysfunction showed a significantly lower expression of red cell eNOS compared to aged-matched healthy individuals (Fig. 5A; mean red cell eNOS expression was 0.519 ± 0.083 vs. 1.058 ± 0.55, unpaired T-test $p < 0.0001$). Furthermore, univariate regression analysis revealed that erythrocytic eNOS expression correlated with endothelial function in humans ($R^2 = 0.318$ $F=12.144$ $p=0.002$) (Fig. 5A). Red cell eNOS activity was measured in a randomized subgroup of the study population by analyzing the conversion of ^{14}C-Arginine into ^{14}C-Citrulline catalyzed by the isolated protein (Fig. 5B). We found that red cell eNOS activity was also significantly decreased in patients with endothelial dysfunction as compared to the healthy control group ($p= 0.0337$, unpaired t-test) (Fig 5B). Taken together, these results indicate that human red cell eNOS activity mirrors vascular endothelial function.

Discussion

The key findings of our study are: 1) formation of NO and related nitrosative species occurs constitutively in all subtypes of human blood cells, with cell-specific intensity differences; 2) intracellular NO formation can be visualized in RBCs using diaminofluoresceins despite the abundance of the NO scavenger oxyhemoglobin and the nitrosation scavengers glutathione and ascorbate; 3) human RBCs contain a catalytically active version of the classical endothelial NOS isoform (eNOS, NOS3) that converts L-arginine to L-citrulline in a Ca^{2+}/calmodulin-dependent manner; 4) both expression and activity of red cell eNOS are compromised in CAD patients; and 5) the extent of eNOS impairment in RBCs correlates with the degree of endothelial dysfunction, demonstrating disease relevance of this blood cell derived NO activity.

Visualization of NO formation in blood cells and fluorescent probe chemistry.
By comparing intracellular fluorescence intensities of different cell subpopulations from the same blood sample loaded with DAF-FM diacetate, almost the same fluorescence intensity was apparent in RBCs as in lymphocytes, and only ~2-3 fold lower values than in neutrophils (granulocytes) or monocytes. In blood of healthy individuals, the number of RBCs is about 3 orders of magnitude higher than the number of white cells. Our findings thus indicate that in the human circulation, RBCs not only transport the bulk of nitrite, the major intravascular NO storage form that becomes bioactivated under hypoxic conditions[35], but also represent the largest cellular compartment in which NO is produced under normoxic conditions.

Although diaminofluoresceins are the most frequently used and best investigated NO imaging probes[36;37], they do not react with NO directly. Initially, it was proposed that DAF-derivatives might interact with reactive nitrosating species derived from the reaction of NO with O_2 such as N_2O_3[38] or nitrous acid [39], to form intermediary N-nitrosamines that are subsequently converted to the highly fluorescent triazole derivatives, DAF-2T or DAF-FM-T[37]. However N_2O_3 is not likely to be formed efficiently in aqueous biological environments, except in lipid membranes[40]. Therefore, Wardman[40] argued that DAFs may undergo one-

electron oxidation to an anilinyl radical that subsequently reacts with NO in a radical-radical reaction. Both mechanisms are probably operating in concert inside cells. While the former may explain the abundance of DAF-FM related fluorescence in membrane-rich compartments, the latter complicates the interpretation of results solely based on DAF-FM related fluorescence due to dependence of the latter on ROS formation. Since RBCs are particularly rich in the NO-scavenger hemoglobin while also containing high concentrations of antioxidants, capable of scavenging nitrosating intermediates and/or reducing the oxidized probe, effective intracellular dye accumulation[28] probably accounts for the ability of diaminofluoresceins to detect NO intracellularly. Nevertheless, its detection in the vicinity of millimolar Hb in RBCs would seem to be reason enough to question the universal validity of the classical "hemoglobin NO-scavening paradigm" (see below).

Origin of constitutive NO synthesis within RBCs.

Using an advanced multi-level analytical approach we here provided unequivocal evidence for the conversion of DAF-FM into DAF-FM-T by NO formed by RBCs under normoxic conditions. RBCs contain both a constitutive Ca^{2+}-dependent NOS containing epitopes of an eNOS[6;15;16;25] and an active XOR[6]. Thus, enzymatic NO synthesis in RBCs might occur either via NOS-catalyzed L-arginine to citrulline conversion[15;16;18] or by XOR-mediated nitrite reduction[6;12;41]. We found that no DAF-FM-T was formed in the presence of the specific NOS inhibitors L-NAME and L-NIO, or by treating RBCs with $Fe[DETC]_2$, which is commonly used as NO spin-trap in ESR studies [27]. Similar results were obtained using flow cytometry. RBC preincubation with nitrite under normoxic conditions did not affect intracellular fluorescence either, ruling out a major role for nitrite in normoxic NO production detectable by DAF-FM. At pH 5.5 higher concentrations of nitrite (> 200 µM) strongly increased intracellular fluorescence. Collectively, these results demonstrate that under normoxic conditions constitutive NO production in RBCs is largely NOS-dependent, while under hypoxic conditions it may involve nitrite reduction by deoxyhemoglobin[5;11], XOR, carbonic anydrase[13] and/or eNOS itself[6;12].

Activity of a red cell NOS may be involved in the regulation of RBC lifespan[42], deformability[16;43 44], and potentially red cell velocity and blood flow[44]. This notion is in line with previous findings showing that NOS inhibitors abolish the anti-platelet effects of RBCs in vitro[15;16] and decrease the level of NO products released by isolated RBCs[16;24], however do not affect intracellular nitrite concentrations[45]. Thus RBCs may also contribute to vascular homeostasis, independent of their "classical role" as transporters of oxygen, energy substrates and nutrients. Given the contribution RBCs make to the circulating NO pool and their role in hypoxic vasodilation[46] further studies are warranted to address its functional significance for the regulation of RBC function and beyond.

Isolation, isoform identification and activity of red cell eNOS.

Previous studies have used antibodies directed against eNOS and iNOS epitopes for western blotting or immunocytochemistry to probe for the presence of a NOS in RBCs and activity assays to measure either the RBC-dependent conversion of radiolabelled arginine into citrulline or the formation of NO oxidation products. Deliconstantinos *et al.* isolated the protein by affinity chromatography using NADPH-binding protein affinity columns and measured L-NAME sensitive nitrite production by RBCs using a modified Griess reaction[19]. Using immunohistochemistry, Jubelin *at al.* found a protein that cross-reacted with antibodies directed against calmodulin, eNOS and iNOS[25] whereas western blot analysis of RBC lysates[15;20] and membranes[6;16] confirmed the presence of a protein with eNOS epitopes. Two groups hypothesized that RBCs express a novel NOS isoform[23;25], but no sequence confirmation analysis was provided.

The main technical hurdle in the biochemical characterization of proteins in RBCs is the presence of overwhelmingly high level of hemoglobin, which represents a formidable obstacle to purification, activity determination, immunostaining, and colorimetric/fluorimetric assay. In this study, we chose to isolate NOS from hemolysates under native conditions to permit combined structural and functional analysis. After purification of calmodulin-binding enzyme by affinity chromatography and immunoprecipitation using anti-eNOS antibodies, we

identified a 130kD-band by SDS-PAGE, indicating that red cell NOS contains both a calmodulin binding site and eNOS-like epitopes. Similar results were obtained when immunoprecipitation was performed directly from crude RBC lysates using different antibodies. While these results strongly suggested that the 130kD band isolated from RBCs was indeed an eNOS protein, further analyses were performed to obtain peptide sequences of tryptic digests by LC-MS/MS. Obtaining the sequence of four different peptides from two independent analyses permitted unequivocal identification of the protein as the classical eNOS (NOS3) isoform. Two of the four sequenced peptides aligned with 100% homology to the C-terminal region of eNOS, which is absent in the NOS3A-C splice variants. Less homology was observed with the sequences related to nNOS (NOS1) and iNOS (NOS2). We thus conclude that RBCs contain eNOS, the same protein that is constitutively expressed in endothelial cells. Two earlier studies suggested that RBCs also contain iNOS[20;25]. We are unable to confirm these reports as we failed to isolate any iNOS from crude human RBC lysates of healthy donors using specific anti-NOS2 antibodies for immunoprecipitation.

While a L-NNA/L-NAME-inhibitable NOS activity has been demonstrated by measuring NO metabolites or citrulline in the supernatant of intact erythrocytes[15;16;19 2;16] and RBC membranes[16;23], two reports suggested RBCs harbor an inactive NOS.[20;34] It was important to confirm, therefore, that the protein identified as eNOS in our study was catalytically active, L-arginine:citrulline conversion was dependent on the presence of Ca^{2+}/calmodulin, and activity was inhibited by L-NAME. While we cannot exclude the additional presence of minor amounts of other NOS isoforms in RBCs it appears that the majority of NO produced in these cells is generated by an active eNOS.

Is red cell eNOS of relevance to cardiovascular disease?

Perhaps one of the most surprising results from our studies is that red cell eNOS expression and activity significantly correlate with flow-mediated dilation, a diagnostic marker of endothelial function and eNOS activity. Similarly to endothelial eNOS dysfunction, red cell

eNOS dysfunction may dependent on both decreased protein levels, and changes in regulation/catalytic activity. Impaired endothelial function, decreased eNOS activity and/or NO bioavailability are conditions strongly related to cardiovascular disease[26;47] Thus, a systemic eNOS deficiency and/or dysfunction appears to prevail in patients with cardiovascular disease the consequences of which are not limited to impaired vascular function, but may also affect function of platelets[48] and red blood cells.

A central challenge of any hypothesis proposing a role of RBC-derived NO in human (patho)physiology is to understand how NO formed by these cells can escape irreversible dioxygenation reaction with oxyhemoglobin, a rapid reaction known to convert NO to nitrate. A “metabolon complex” of deoxyhemoglobin, AE/band 3, carbonic anhydrase, aquaporin and Rh-protein channels was proposed to explain nitrite protonation and may serve to facilitate the export of NO or its metabolites.[49] The localization of eNOS-immunoreactivity on the cytoplasmic side of the RBC membrane, as detected by immunogold-labelling and electron microscopy imaging[16], supports the notion that the RBC membrane plays a central role in this process, possibly by effectively “compartmentalizing” NO production, signalling and scavenging machinery. Our results invite a rethink about the role of hemoglobin in NO biology, inasmuch as its oxygenated form is considered an NO scavenger under any condition. Several factors have been identified that explain why endothelial NO escapes scavenging by hemoglobin[8;11;46;49;50], but those discussions did not consider the possibility that NO might be produced in RBCs themselves. The observation that NO formation can be detected in the vicinity of abundant oxyhemoglobin would seem to warrant a careful reassessment of this universally accepted paradigm.

Summary and Outlook

Only recently indices of RBC number, size, and function have emerged as independent risk factors of cardiovascular disease[1-3]. Besides endothelial cells RBCs may also contribute to NO-dependent regulation of vascular homeostasis. Our present findings suggest that red cell eNOS activity might serve the purpose of compensating for NO trapping by providing an

efficient “NO shield” that maintains effective intracellular signalling. Moreover, red cell eNOS expression/activity might be a complementary diagnostic tool to assess vascular homeostasis and provide new therapeutic strategies for fighting cardiovascular disease.

Acknowledgement

This work was supported by the Deutsche Forschungsgemeinschaft (DFG 405/5-1 and FOR809 TP7 Me1821/3−1), the Anton Betz Stiftung, (26/2010), the Susanne-Bunnenberg-Stiftung at Düsseldorf Heart Center to MK, and the Forschungskommission of the Medical Faculty of the Heinrich-Heine-University Düsseldorf to MCK. LC-MS analyses were conducted at the Chemical Analytical Facility, University of Reading. We wish to thank Katharina Lysaja for indispensable technical assistance, Profs. Victoria Kolb-Bachofen, Dieter Häussinger, and Jeremy Spencer for allowing us to use the FluostarOPTIMA, the FACS Canto II flow cytometer, and the HPLC, respectively, and Prof. Axel Gödecke for offering us to use his radioisotope facility.

Authorship

MCK planned and executed experiments, analyzed data, and drafted the manuscript; ARM performed HPLC; RS, recruited patients, measured FMD, GGK, ran LC-MS/MS for DAF-FM; LS,TK, PH performed experiments; CK, carried out peptide sequencing; CH assisted with the study plan; KDK, provided essential materials and intellectual input; NH provided essential intellectual input; MF, provided conceptual and intellectual input and wrote the manuscript, MK planned the study and wrote the manuscript. All authors have no conflict of interest to declare.

References

1. Anand IS, Kuskowski MA, Rector TS, et al. Anemia and change in hemoglobin over time related to mortality and morbidity in patients with chronic heart failure: results from Val-HeFT. *Circulation* 2005;112(8):1121-1127.

2. Kulier A, Levin J, Moser R, et al. Impact of preoperative anemia on outcome in patients undergoing coronary artery bypass graft surgery. *Circulation* 2007;116(5):471-479.

3. Sabatine MS, Morrow DA, Giugliano RP, et al. Association of hemoglobin levels with clinical outcomes in acute coronary syndromes. *Circulation* 2005;111(16):2042-2049.

4. Moncada S, Palmer RMJ, Higgs EA. Nitric oxide, biology pathophysiology and pharmacology. *Pharmacol Rev* 1991;43:109-142.

5. Cosby K, Partovi KS, Crawford JH, et al. Nitrite reduction to nitric oxide by deoxyhemoglobin vasodilates the human circulation. *Nat Med* 2003;9(12):1498-1505.

6. Webb A, Milsom A, Rathod K, et al. Mechanisms underlying erythrocyte and endothelial nitrite reduction to nitric oxide in hypoxia: role for xanthine oxidoreductase and endothelial nitric oxide synthase. *Circ Res* 2008;103(9):957-964.

7. Herold S. The outer-sphere oxidation of nitrosyliron(II)hemoglobin by peroxynitrite leads to the release of nitrogen monoxide. *Inorganic chemistry* 2004;43(13):3783-3785.

8. Jia L, Bonaventura C, Bonaventura J, et al. S-nitrosohaemoglobin: a dynamic activity of blood involved in vascular control. *Nature* 1996;380:221-226.

9. Gladwin MT, Lancaster jr JR, Freeman BA, et al. Nitric oxide's reactions with hemoglobin: a view through the SNO-storm. *Nat Med* 2003;9:496-500.

10. Rassaf T, Bryan NS, Maloney RE, et al. NO adducts in mammalian red blood cells: too much or too little? *Nat Med* 2003;9:481-482.

11. Nagababu E, Ramasamy S, Albernethy R, et al. Active nitric oxide produced in the red cell under hypoxic conditions by deoxyhemoglobin-mediated nitrite reduction. *J. Biol Chem.* 2003;278:46349-46356.

12. Zweier JL, Wang P, Samouilov A, et al. Enzyme-independent formation of nitric oxide in biological tissues. *Nat Med* 1995;1(8):804-809.

13. Aamand R, Dalsgaard T, Jensen FB, et al. Generation of nitric oxide from nitrite by carbonic anhydrase: a possible link between metabolic activity and vasodilation. *Am J Physiol Heart Circ Physiol* 2009;297(6):H2068-H2074.

14. Ellsworth ML, Forrester T, Ellis CG, et al. The erythrocyte as a regulator of vascular tone. *Am J Physiol Heart Circ Physiol* 1995;269(6):H2155-H2161.

15. Chen LY, Mehta JL. Evidence for the presence of L-arginine-nitric oxide pathway in human red blood cells: relevance in the effects of red blood cells on platelet function. *J Cardiovasc Pharmacol* 1998;32:57-61.

16. Kleinbongard P, Schulz R, Rassaf T, et al. Red blood cells express a functional endothelial nitric oxide synthase. *Blood* 2006;107(7):2943-2951.

17. Sprague RS, Stephenson AH, Dimmitt RA, et al. Effect of L-NAME on pressure-flow relationships in isolated rabbit lungs: role of red blood cells. *Am J Physiol* 1995;269:H1941-H1948.

18. Yang BC, Nichols WW, Mehta JL. Cardioprotective effects of red blood cells on ischemia and reperfusion injury in isolated rat heart: release of nitric oxide as a potential mechanism. *J Cardiovasc Pharmacol Therapeut* 1996;1:297-305.

19. Deliconstantinos G, Villiotou V, Stavrides JC, et al. Nitric oxide and peroxynitrite production by human erythrocytes: a causative factor of toxic anemia in breast cancer patients. *Anticancer Res.* 1995;15:1435-1446.

20. Kang ES, Ford K, Grokulsky G, et al. Normal circulating adult human red blood cells contain inactive NOS proteins. *J Lab Clin Med* 2000;135:444-451.

21. Metha JL, Metha P, Li D. Nitric oxide synthase in adult red blood cells: vestige of an earlier age or a biologically active enzyme? *J Lab Clin Med* 2000;135:430-431.

22. Bohmer A, Beckmann B, Sandmann J, et al. Doubts concerning functional endothelial nitric oxide synthase in human erythrocytes. *Blood* 2012;119(5):1322-1323.

23. Bhattacharya S, Chakraborty PS, Basu RS, et al. Purification and properties of insulin-activated nitric oxide synthase from human erythrocyte membranes. *Arch Physiol Biochem* 2001;109(5):441-449.

24. Mihov D, Vogel J, Gassmann M, et al. Erythropoietin activates nitric oxide synthase in murine erythrocytes. *Am J Physiol Cell Physiol* 2009;297(2):C378-C388.

25. Jubelin BC, Gierman JL. Erythrocytes may synthesize their own nitric oxide. *AJH* 1996;9:1214-1219.

26. Heiss C, Lauer T, Dejam A, et al. Plasma nitroso compounds are decreased in patients with endothelial dysfunction. *JACC* 2006;47:573-579.

27. Kleschyov AL, Mollnau H, Oelze M, et al. Spin trapping of vascular nitric oxide using colloid Fe(II)-diethyldithiocarbamate. *Biochem Biophys Res Commun* 2000;275(2):672-677.

28. Rodriguez J, Specian V, Maloney R, et al. Performance of diamino fluorophores for the localization of sources and targets of nitric oxide. *Free Radic Biol Med* 2005;38(3):356-368.

29. Giblett E, Anderson J. Electrophoretic analysis of polymorphic red cell enzymes. In: Red cell metabolism. Beutler, E. Edinburgh: Churchill Livingstone, 1986;108-123.

30. Cortese MM, Suschek CV, Wetzel W, et al. Zinc protects endothelial cells from hydrogen peroxide via Nrf2-dependent stimulation of glutathione biosynthesis. *Free Radic Biol Med.* 2008;44(12):2002-2012.

31. Kang D, Gho YS, Suh M, et al. Highly sensitive and fast protein detection with coomassie brilliant blue in sodium dodecyl sulfate-polyacrylamide gel electrophoresis. I *Bull Korean Chem Soc*. 23(11), 1511-1512. 2002.

32. Bredt DS, Schmidt HHHW. The citrullin assay. In: Methods in nitric oxide research. Feelisch M, Stamler JS, eds. 1996;249-255.

33. Jourd'heuil D. Increased nitric oxide-dependent nitrosylation of 4,5-diaminofluorescein by oxidants: implications for the measurement of intracellular nitric oxide. *Free Radic Biol Med.*2002;33(5):676-684.

34. Bähmer A, Beckmann B, Sandmann J, et al. Doubts concerning functional endothelial nitric oxide synthase in human erythrocytes. *Blood* 2012;119(5):1322-1323.

35. Dejam A, Hunter CJ, Pelletier MM, et al. Erythrocytes are the major intravascular storage sites of nitrite in human blood. *Blood* 2005;106(2):734-739.

36. Hong H, Sun J, Cai W. Multimodality imaging of nitric oxide and nitric oxide synthases. *Free Radic Biol Med.* 2009;47(6):684-698.

37. Nagano T, Yoshimura T. Bioimaging of nitric oxide. *Chem Rev* 2002;102(4):1235-1270.

38. Nakatsubo N, Kojima H, Kikuchi K, et al. Direct evidence of nitric oxide production from bovine aortic endothelial cells using new fluorescence indicators: diaminofluoresceins. *FEBS Letters* 1998;427(2):263-266.

39. Williams DL. *Nitrosation reactions and the chemistry of nitric oxide.* Elsevier, 2004.

40. Wardman P. Fluorescent and luminescent probes for measurement of oxidative and nitrosative species in cells and tissues: progress, pitfalls, and prospects. *Free Radic Biol Med.* 2007;43(7):995-1022.

41. Godber BLJ, Doel JJ, Sapkota GP, et al. Reduction of Nitrite to Nitric Oxide Catalyzed by Xanthine Oxidoreductase. *J Biol Chem* 2000;275(11):7757-7763.

42. Lang KS, Lang PA, Bauer C, et al. Mechanisms of suicidal erythrocyte death. *Cell Physiol Biochem.* 2005;15(5):195-202.

43. Bor-Kucukatay M, Wenby RB, Meiselman HJ, et al. Effects of nitric oxide on red blood cell deformability. *Am J Physiol Heart Circ Physiol* 2003;284:H1577-H1584.

44. Horn P, Cortese-Krott MM, Keymel S, et al. Nitric oxide influences red blood cell velocity independently of changes in the vascular tone. *Free Radic Res.* 2011;45(6):653-661.

45. Vitturi DA, Teng X, Toledo JC, et al. Regulation of nitrite transport in red blood cells by hemoglobin oxygen fractional saturation. *Am J Physiol Heart Circ Physiol* 2009;296(5):H1398-H1407.

46. Crawford JH, Isbell TS, Huang Z, et al. Hypoxia, red blood cells, and nitrite regulate NO-dependent hypoxic vasodilation. *Blood* 2006;107(2):566-574.

47. Rassaf T, Heiss C, Hendgen-Cotta U, et al. Plasma nitrite reserve and endothelial function in the human forearm circulation. *Free Radic Biol Med.* 2006;41(2):295-301.

48. Gkaliagkousi E, Ritter J, Ferro A. Platelet-derived nitric oxide signaling and regulation. *Circ Res* 2007;101(7):654-662.

49. Gladwin MT, Schechter A, Kim-Shapiro DB, et al. The emerging biology of the nitrite anion in signaling, blood flow and hypoxic nitric oxide homeostasis. *Nat Chem Biol* 2005;1:308-314.

50. Kim-Shapiro DB, Schechter AN, Gladwin MT. Unraveling the reactions of nitric oxide, nitrite, and hemoglobin in physiology and therapeutics. *Arterioscler Thromb Vasc Biol* 2006;26(4):697-705.

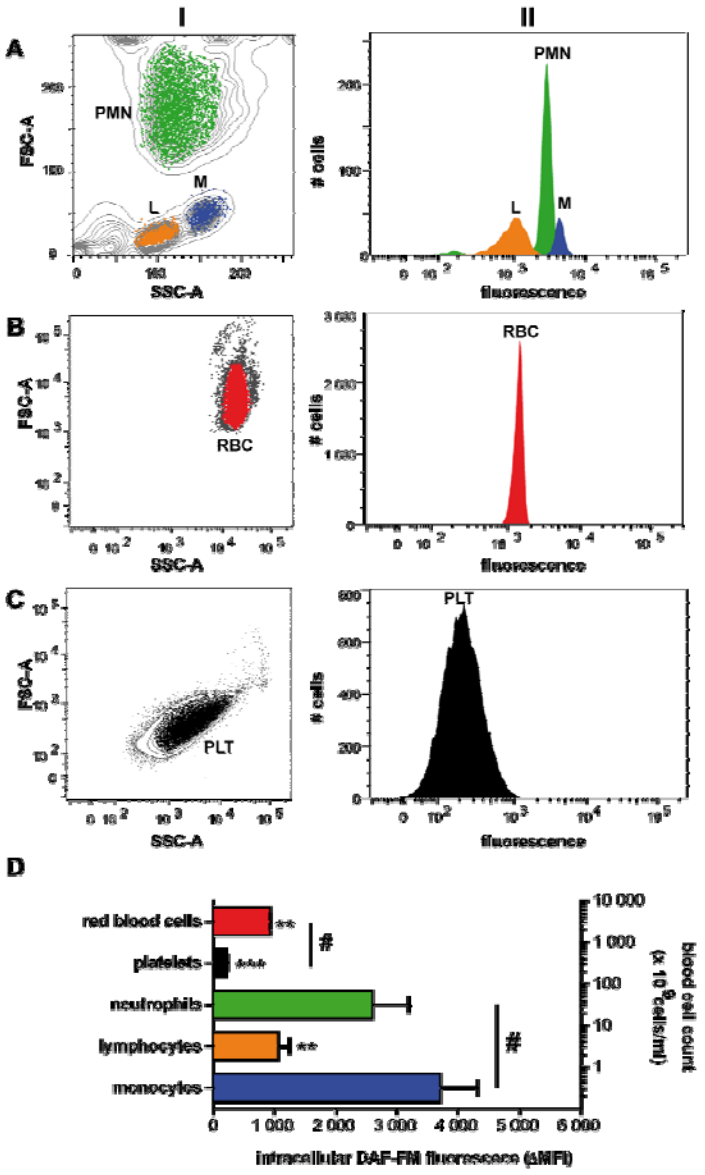

Figure 1: Hierarchy of DAF-FM-associated fluorescence intensity in human blood cells. (A-C) Blood was separated into platelet-rich plasma, leukocytes and red blood cell fractions and loaded with DAF-FM diacetate. Blood cell subpopulations within each fraction were identified by flow cytometry on the basis of their FSC/SSC distribution (panels I) and by surface marker discrimination (not shown). The distribution of the green fluorescence signal measured in each gate is depicted in panels II. L-lymphocytes, M-macrophages, PLT-platelets, PMN-polymorphonuclear granulocytes, RBC-red blood cells; SSC-side scatter, FSC-forward scatter. (D) Specific intracellular fluorescence of blood cell subpopulations

(assessed as ΔMFI = median fluorescence intensity - background fluorescence) plotted in relation to blood composition (i.e., relative levels of each cell in blood; right y-axis) (n=4; ANOVA p= 0.0002: Bonferroni vs. monocytes **p< 0.01; ***p<0.001, # T-Test p<0.001).

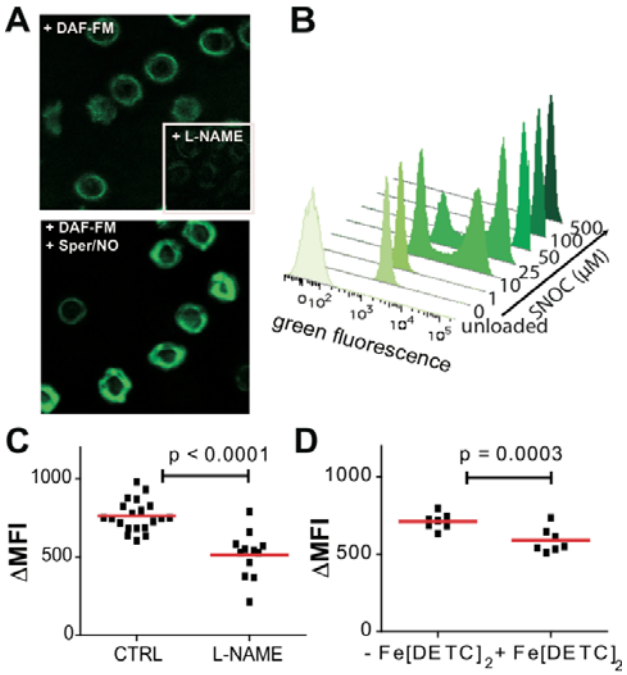

Figure 2: Visualization of intracellular NO production in RBCs. (A) Laser scanning micrographs of RBCs loaded with DAF-FM before (top) or after pre-treatment with 3 mM L-NAME (inset) and further incubation with 100 µM Sper/NO (bottom). (B) Fluorescence distribution plot of untreated cells (front lane), cells loaded with DAF-FM only (second lane), or further treated with 1-500 µM SNOC (other lanes). Representative data from 6 experiments (C) Decrease in intracellular RBC fluorescence (ΔMFI) as assessed by flow cytometry following treatment with the NOS inhibitor L-NAME. (D) Intracellular RBC fluorescence (ΔMFI) after treatment with the NO scavenger $Fe[DETC]_2$. ΔMFI = median fluorescence intensity - background fluorescence.

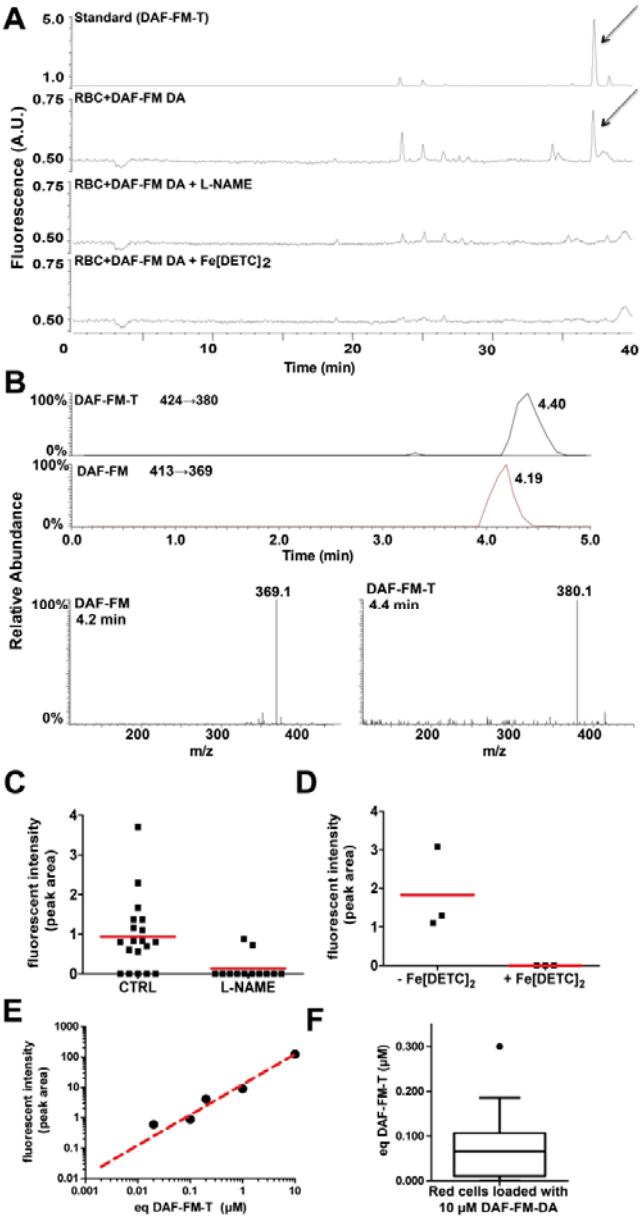

Figure 3: Suppression of NOS-mediated constitutive DAF-FM-T formation within RBCs after inhibition of NO synthesis or NO scavenging. (A) RBCs were left either untreated or pretreated with the specific NOS inhibitor L-NAME or the NO scavenger $Fe[DETC]_2$, washed, loaded with DAF-FM diacetate and analyzed by HPLC with fluorescence detection. (B) RBCs were treated as described in A and analyzed by LC-MS; The upper panel show the mass spectrum of the respective peaks at 4.2 min for DAF-FM and 4.4 min for DAF-FM-T. The bottom panels shows the SRM chromatograms for DAF-FM-T, monitoring the

fragmentation from 424 to 380 due to the loss of a CO_2 from the parent molecule, and DAF-FM monitoring the transition from 413 to 369. (C, D) DAF-FM-T related peak areas from 3-5 independent experiments with different blood donors; samples treated as in A. (E, F) Estimation of the DAF-FM-T quantities formed by constitutive NOS activity in RBCs; E: regression curve obtained by diluting DAF-FM-T standards in RBC lysates. Measured peak areas were plotted against DAF-FM-T concentrations, assuming 100% conversion of DAF-FM into DAF-FM-T. F: Calculated DAF-FM-T equivalents (eq) formed in ~10^7 red cells loaded with DAF-FM diacetate and incubated for 30 min RT. After removing the outlier (according to Tuckey, see box plot) the mean DAF-FM-T concentration in RBC was 64±12 nM (n= 19).

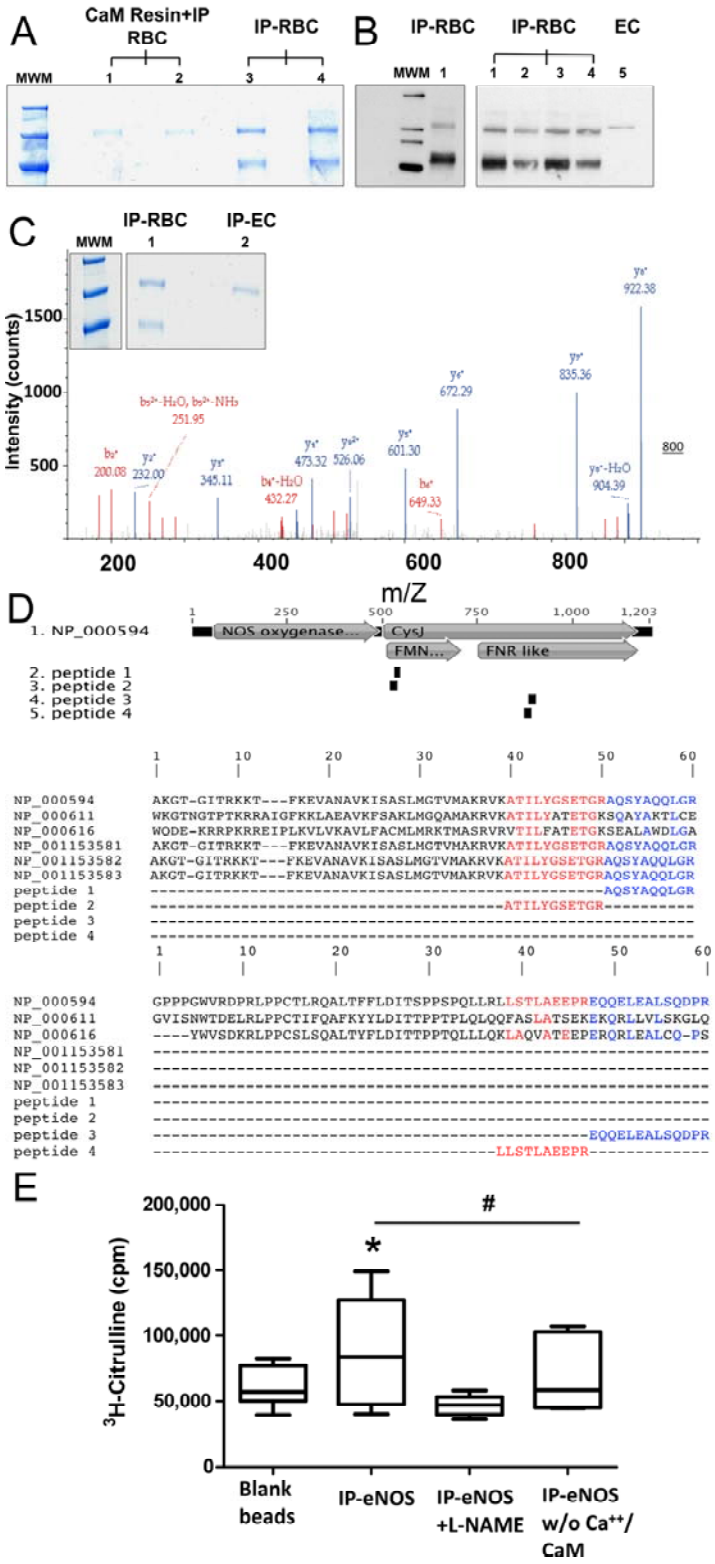

Fig. 4: Human RBCs contain an active NOS3. A) Constitutive NOS (130 kD) was isolated from human RBCs by affinity chromatography with a calmodulin (CaM)-binding column

followed by immunoprecipitation (IP) with a mouse anti-human NOS3 or directly by immunoprecipitation from crude RBC lysates (lanes 1 and 2 as well as 3 and 4 are independent samples) **B)** The NOS enzyme was isolated directly from crude red cell lysates by immunoprecipitation with a mouse anti-human eNOS antibody and analyzed by Western blotting. As a control a crude EC lysate was loaded in lane 5 (MWM = molecular weight marker). **C)** Coomassie gel used for identification purposes and representative example of peptide identification by LC-MS/MS sequencing; depicted is the fragmentation spectrum of the peptide AQSYAQQLGR. **D)** Alignment of peptides identified by LC-MS/MS with sequences of nNOS, iNOS and all known eNOS splice variants. Top panel: Peptides 1 and 2 aligned within the FMN reductase-like region (FMN binding region), while peptides 3 and 4 aligned with the ferredoxin reductase (FNR)-like region (FAD and NADPH binding region). CysJ = Sulfite reductase, alpha subunit (flavoprotein) region. NOS oxygenase: nitric oxide synthase eukaryotic oxygenase domain.Bottom panels: The sequences shown in detail and compared with the other NOS isoforms. The sequences of the peptides are identical with NOS3, isoform 1 only. NP_000611 = NOS1, nNOS, NP000616= NOS2, iNOS, NP_000594 = NOS3, isoform 1. Splice variants of NOS3 are NP_001153581 = NOS3, isoform 2, NP_001153582 = NOS3, isoform 3, NP_001153583 = NOS3, isoform 4. **E)** Activity of immunoprecipitated red cell eNOS. The activity of NOS3 immunoprecipitated from RBCs was assessed by measuring the conversion of L-^{3}H-arginine to L-^{3}H-citrulline. Total radioactivity is expressed as counts per minute (cpm). (ANOVA p=0.0447; Tukey IP vs. IP+L-NAME *p<0.05; # IP vs. Ca^{++}/CaM T-Test p=0.0394)

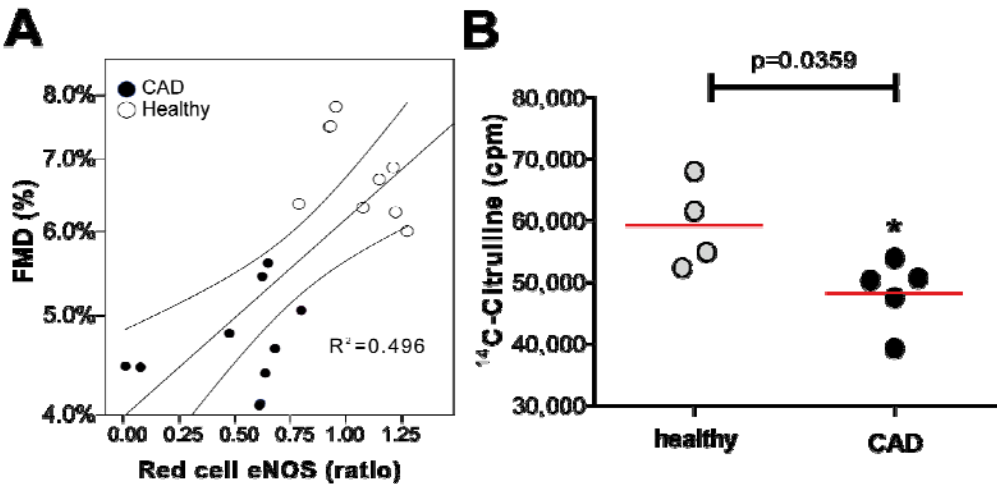

Fig.5: Changes in the red cell eNOS expression and activity in patients with endothelial dysfunction. A) Monovariate linear correlation analysis between red cell eNOS expression as evaluated by western blot analysis (see supplemental information) and endothelium-dependent flow mediated dilation (FMD) in patients affected with endothelial dysfunction and healthy individuals (healthy); B) The activity of red cell eNOS was evaluated in a randomized subset of the groups by evaluating the conversion of ^{14}C-L-arg into ^{14}C-L-citrulline. Total radioactivity is expressed as counts per minute (cpm); T-Test * p = 0.0359